

***Didymium*-like myxogastrids (class Mycetozoa) as endocommensals of sea urchins (*Sphaerechinus granularis*)**

Iva Dyková^{1,2}, Jiří Lom¹, Helena Dvořáková¹, Hana Pecková¹ and Ivan Fiala^{1,2}

¹Institute of Parasitology, Biology Centre, Academy of Sciences of the Czech Republic, Branišovská 31, 370 05 České Budějovice, Czech Republic;

²Faculty of Biological Sciences, University of South Bohemia, Branišovská 31, 370 05 České Budějovice, Czech Republic

Key words: *Didymium*-like myxogastrids, Myxogastrea, sea-urchin amoeba strains, SSU rDNA, flagellar apparatus, phylogeny

Abstract. This paper sums up the results of light microscopical, ultrastructural and molecular studies of five strains of amoeboid organisms isolated as endocommensals from coelomic fluid of sea urchins, *Sphaerechinus granularis* (Lamarck), collected in the Adriatic Sea. The organisms are reported as *Didymium*-like myxogastrids. Of the life-cycle stages, the attached amoeboids, flagellated trophozoites, cysts and biflagellated swimmers are described. Formation of fruiting bodies was not observed. Although phylogenetic analyses of SSU rDNA sequences indicated a close relationship with *Hyperamoeba dachnaya*, our sea-urchin strains have not been assigned to the genus *Hyperamoeba* Alexeieff, 1923. The presence of either one or two flagella reported in phylogenetically closely related organisms and mutually distant phylogenetic positions of strains declared as representatives of the genus *Hyperamoeba* justify our approach. Data obtained in this study may be useful in future analyses of relationships of the genera *Didymium*, *Hyperamoeba*, *Physarum* and *Pseudodidymium* as well as in higher-order phylogeny of Myxogastrea.

The interest in amoebic diseases of invertebrates recently renewed by outbreaks associated with mass mortalities in American lobsters in Long Island Sound, USA (Mullen et al. 2004, 2005), as well as continuing research of Amoebic Gill Disease (AGD) in farmed fish, inspired isolation attempts focused on *Paramoeba*/*Neoparamoeba* spp. as potential agents of infections in invertebrates including sea urchins. Mass mortalities of echinoids attributed to *Paramoeba invadens* Jones, 1985 infections were reported in the green sea urchin *Strongylocentrotus droebachiensis* along the Atlantic coast of Nova Scotia, Canada, between 1980 and 1983 (Jones 1985).

Since the number of amoeboid organisms isolated from invertebrates and stored in culture collections is rather limited, we have characterized several strains isolated from the first set of sea urchins we have sampled thus far. None of the isolated strains could be assigned to *Paramoeba*/*Neoparamoeba* species searched for; most of isolated strains were mutually similar and interesting enough to be presented in this study.

MATERIALS AND METHODS

Five strains of amoeboid organisms presented in the study were isolated from 5 out of 34 sea urchins *Sphaerechinus granularis* (Lamarck, 1816) screened for the presence of amphizoic amoebae in their coelomic fluid. Strains were denominated as follows: ECH1, ECH14, ECH43, ECH 49, and ECH54. Sea urchins were collected in the Adriatic Sea, in the nearshore area of the Brač Island (Croatia), in June 2005. Sampling of sea urchins was performed using sterile dispos-

able “self-filling” syringes with needles of 23 gauge designed for bleeding in pigs. Modified malt and yeast extract seawater agar (MY75S in the Catalogue of the UK National Culture Collection 2001) was used for isolation attempts as well as for subculturing of primary isolates, strains and clones. The strength of artificial seawater (Sea salts Sigma S9883) was lowered to 30% and the doses of the extracts to 0.05 g per litre in agar used for primary isolations and initial phases of subculturing. When the growth of bacteria, contaminating all cultures, was balanced, seawater agar with full doses of extracts was used (0.1 g per litre). Cultures were kept at 20°C. About 20 passages were executed before the clonal procedure was completed. Subculturing was done in 10-day intervals.

Our study was aimed at establishing the identity of isolated strains. Morphology of cultured trophozoites, excystment and flagellate transformation were studied in hanging drop preparations using fluid component of the agar medium (30% artificial seawater) and directly in seawater overlay of agar plate cultures. Nomarski differential interference contrast was used to document trophozoites attached to coverslips. (Cultures with no signs of humidity on the surface of agar, in which seawater used for subculturing completely soaked into agar, are in this paper termed “dry” cultures).

In order to compare obviously inactive trophozoites (as observed in agar-plate cultures through Petri dishes), attached cells possessing flagella (as observed in hanging drop preparations), and small flagellate cells displaying fast movements, material for transmission electron microscopy was prepared under two different conditions: 1) Agar plate cultures were fixed *in situ* with cacodylate buffered 2.5% glutaraldehyde, pelleted, postfixed with 1% osmium tetroxide and embedded in Spurr resin. 2) Agar plate cultures were flooded with 5 ml of 30% seawater and then fixed in two steps at four time inter-

vals after their flooding: 5 ml of cacodylate buffered 3% glutaraldehyde were added to the culture flooded with seawater and left to work for 15 min. After that, cells were pelleted, fixed in 2.5% glutaraldehyde for 15 min and postfixed in 1% osmium tetroxide for 45 min. In the course of dehydration, the cells were treated with 1% uranyl acetate dissolved in 75% acetone.

The procedures for cell harvesting and DNA extraction as well as conditions of PCR amplification with universal eukaryotic primers ERIB1 and ERIB10 and sequencing of cloned PCR products have been described earlier (Dyková et al. 2005a, b). The composition of SSU rDNA sequences set (alignment A) prepared to learn phylogeny of strains under study was based on results of our own comparison of light microscopical and ultrastructural features and data obtained from studies of similar organisms (Michel et al. 2003, Walker et al. 2003, Walochnik et al. 2004). After initial analysis, a refined dataset consisting of 13 most closely related sequences and 3 outgroup sequences was assembled (alignment B). SSU rDNA sequences were aligned using Clustal_X program (Thompson et al. 1997). Ambiguously aligned positions including large introns in sequences of *Fuligo septica* (AJ584697), *Pseudodidymum cryptomastigophorum* (AY207466), *Didymium anellus* (AM231292), *D. squamulosum* (AM231293), *D. nigripes* (AF239230), *D. iridis* (AJ938150), *D. iridis* (AJ938151), *D. iridis* (AJ938153) and *D. iridis* (AJ938154) were removed from analyses. The phylogenetic reconstruction of the SSU rDNA sequence data using methods of maximum parsimony (MP), maximum likelihood (ML) and Bayesian inference (BI) followed the practice applied in previous studies (Dyková et al. 2005a, 2006). MP (heuristic search with three bisection-reconnection branch swapping; gaps as missing data; transition/transversion (Ts:Tv) ratio=1:2; bootstrap statistical support with 1 000 replications) and ML (GTR+I+Γ model of evolution; bootstrap statistical support with 500 replications) analyses were performed in the program package PAUP* version 4.0b10 (Swofford 2001). Bayesian analysis using Markov Chain Monte Carlo techniques (GTR+I+Γ model of evolution, 500 000 generations) was inferred with MrBayes v. 3.0 (Ronquist and Huelsenbeck 2003). The nucleotide dissimilarities of SSU rDNA sequences (excluding introns) were calculated from alignment B (2.048 aligned sites).

Phylogenetic analyses were performed to answer the following questions: 1) What are the phylogenetic relationships among strains of amoeboid organisms isolated from sea urchins? 2) What are the phylogenetic relationships of strains from sea urchins to morphologically similar organisms? 3) How ultrastructural features discriminating newly described organisms correlate with phylogeny of organisms under study?

RESULTS

Light microscopy

Agar-plate cultures of sea-urchin strains (SUS) observed in translucent light through Petri dishes, revealed a uniform, dispersed type of growth. Several days after selected cell populations from parent culture had been transferred to a new agar plate, the surface of agar became covered by trophozoites intermingled with cysts.

The density of culture increased gradually up to day 10, when the cysts usually started to outnumber the trophozoites. The formation of fruiting bodies was not observed, not even in attempts to culture SUS using medium recommended for myxogastrids (Emerson YpSs agar 2% with modified contents of yeast protein and soluble starch).

Slight but constant difference in the size of trophozoites was observed during the long period of subculturing in one strain (ECH14/I), compared to the remaining four. The diameter of rounded cysts was $7.5 \pm 0.9 \mu\text{m}$ (strain ECH14/I), $7.7 \pm 1.1 \mu\text{m}$ (ECH 1/I, ECH 43/I and ECH54/I) and $8.0 \pm 1.1 \mu\text{m}$ (ECH49/I), respectively. The percentage of slightly oval cysts was not significant in any of the strains studied.

Morphological similarity of the strains as assumed from observation of agar-plate cultures was confirmed when hanging drop preparations were studied. Contrary to trophozoites in "dry" agar-plate cultures, those washed off the agar surface and left to attach to coverslips possessed flagella (Fig. 1). In addition to the attached, large flagellated forms, individual, small flagellated stages that moved very fast were present in hanging drop preparations. While the number of flagella could be easily distinguished in attached cells, the small size and high speed of locomotion of small flagellated stages did not permit to reveal whether they possessed more than one flagellum. The study of changes, induced by adding 30% seawater in seven-week-old culture of strain ECH49/I (containing exclusively cysts) repeated three times, revealed details of transformation of the life-cycle stages. A minimum of one third of rounded cysts changed their shape into oval within 1 hr after the seawater was added to the culture. Simultaneously, conspicuous movements inside these cysts were observed. Subsequent liberation of flagellated stages from cysts was completed in 15 min. In the culture overlaid with 30% seawater, the number of small flagellated stages grew progressively in the course of 3 hrs. Later on, small flagellated stages slowed down their locomotion, attached to the surface of agar and transformed into amoeboid trophozoites of irregular shape. The process of exflagellation was observed also in "resting" trophozoites in "dry" agar-plate cultures when covered with seawater.

Transmission electron microscopy

Trophozoites of SUS from "dry" cultures fixed *in situ* several times in the course of subculturing resembled those of other free-living naked amoebae (Figs. 2, 3). These stages, showing no flagellar activity, had smooth cell surface (Fig. 5), finely granular cytoplasm, only rarely with signs of differentiation into granuloplasm and hyaloplasm, a single nucleus with a distinct nucleolus, numerous mitochondria with tubular cristae and a central, electron-dense core (Fig. 4), endoplasmic reticulum and numerous food vacuoles. The outline of trophozoites was determined by pseudopodial cytoplas-

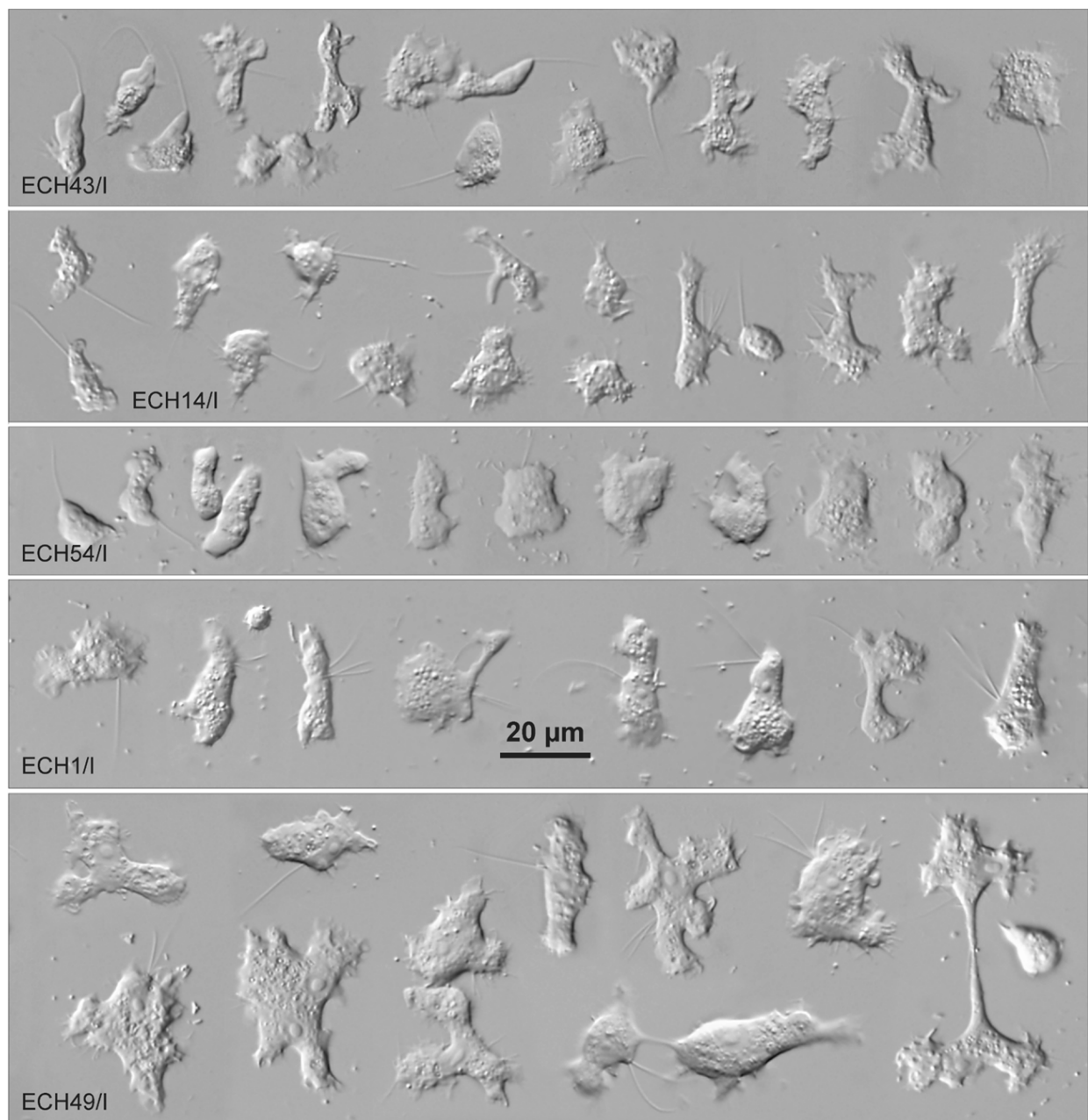


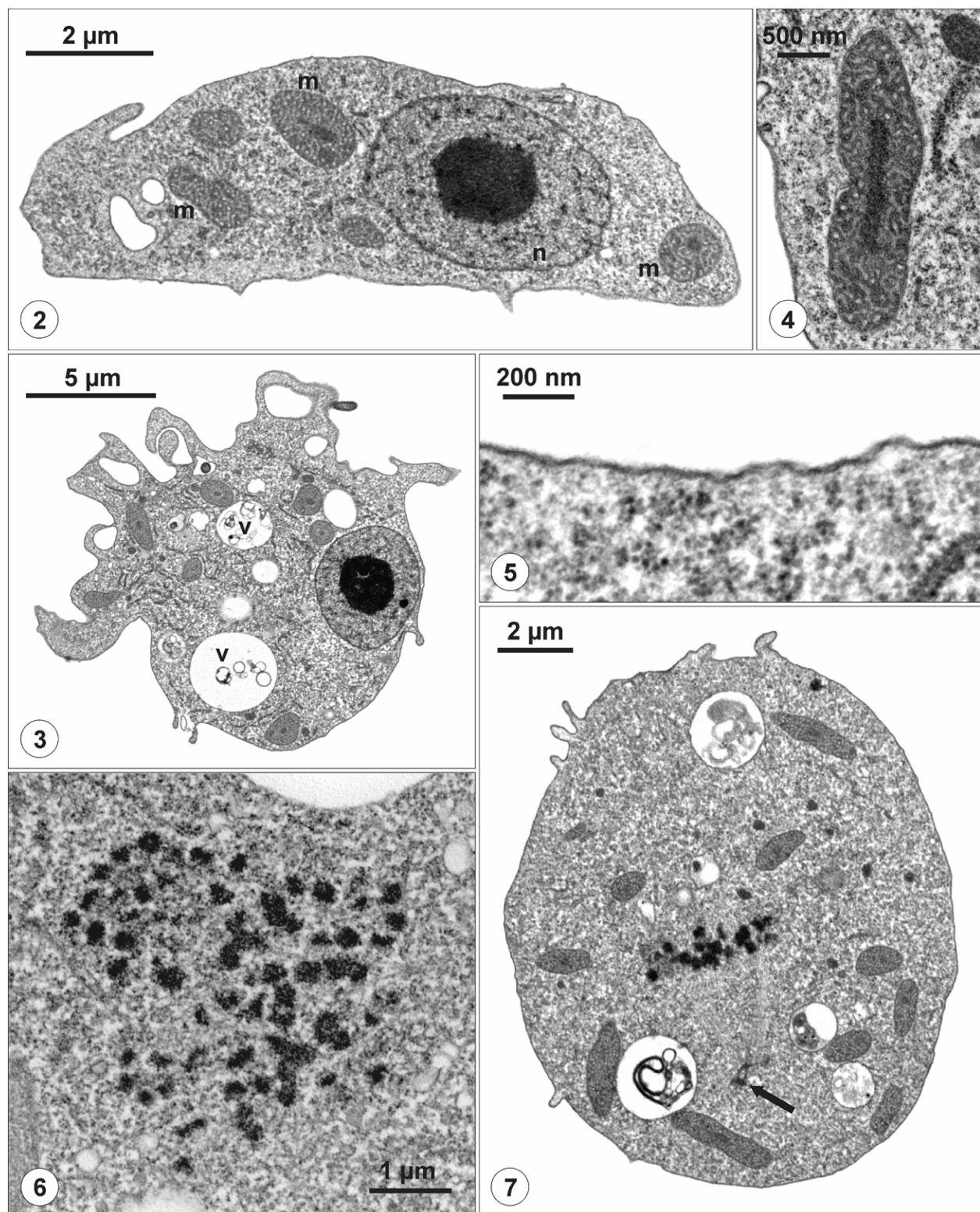
Fig. 1. Trophozoites of sea urchin strains (SUS) washed from agar-plate cultures and observed in hanging drop preparations. Each set of amoeboid organisms represents the most common morphotypes of corresponding clonal culture.

mic projections, sometimes single, sometimes more numerous at the level of sectioning. Flagellar apparatus was not detected in these amoeboid trophozoites although semiserial sections of dozens of them were examined. The cell division proceeded by binary fission. Nuclear division was an open mitosis with non-persisting nuclear envelope (Figs. 6, 7).

The uninucleate cysts (Fig. 8) had a bilayered wall (Fig. 9). The discontinuous and dishevelled outer layer covering cyst wall was observed only exceptionally (Fig. 9). The release of flagellated stages seen in the light microscope was confirmed by transmission electron microscopy (Figs. 10–13).

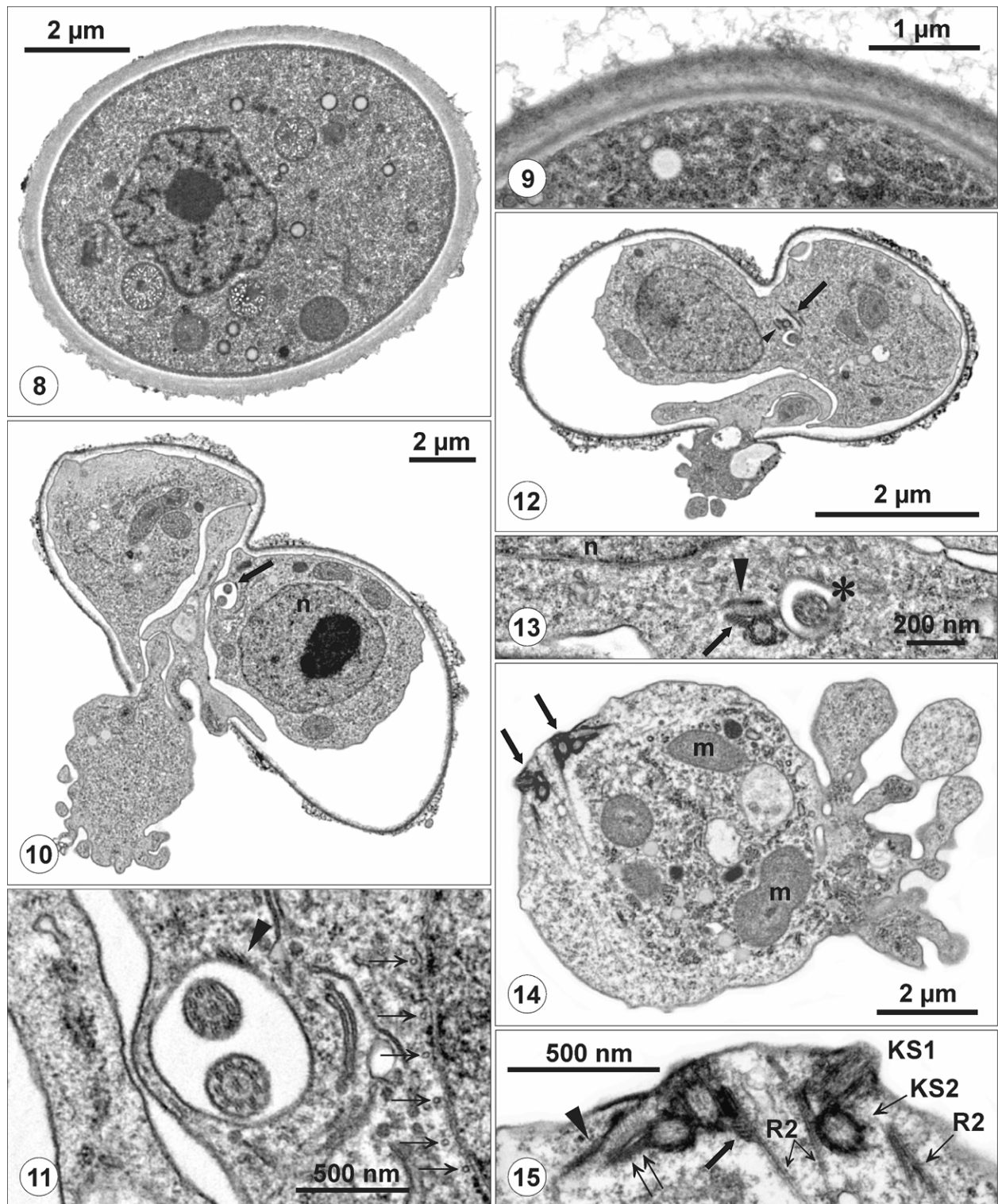
The ultrastructure of amoeboid forms developed under seawater overlay corresponded to the light microscopical observation (Fig. 1). These cells differed substantially from resting trophozoites of “dry” cultures in having flagellar apparatus. They developed into small fast-moving flagellated forms (swarm cells sensu Schuster 1965). These swimmers did not contain food vacuoles, had a pyriform nucleus located near the tapering anterior and flagella-bearing end (Figs. 17, 18). The nucleus had no distinct nucleolus and its envelope displayed nuclear pores of normal structure (Fig. 23).

Flagellar apparatus consisted of two flagella-bearing kinetosomes (KS1, KS2) and associated fibrillar and



Figs. 2, 3. Overview of ultrastructure of trophozoites from “dry” agar-plate culture. m – mitochondrion; n – nucleus; v – food vacuole. **Fig. 4.** Mitochondrion with characteristic central electron-dense core well known in Myxogastrea. **Fig. 5.** Smooth cell surface observed in all life-cycle stages of SUS. **Figs. 6, 7.** Open mitosis observed in trophozoites of SUS. **Fig. 6.** Dispersion of chromatin granules and disappearance of the nuclear envelope. **Fig. 7.** Metaphase in dividing nucleus and centriole (arrow).

Fig. 8. Section of SUS cyst (overview). **Fig. 9.** Bilayered wall in mature cyst. **Fig. 10.** Section through a flagellated stage (the future swarmer) escaping from the cyst. Arrow points at the canal inside which already the two flagella can be seen. **Fig. 11.** Detail of the preceding image. Arrows point at the microtubules of the inner microtubular cone (R1) closely apposed to the



(continued from p. 4) nuclear envelope. Arrowhead marks a constituent of a kinetosome-associated microtubular ribbon. **Fig. 12.** Another future swarmer escaping from the cyst wall. Arrow points at the future complex of kinetosomes KS1 and KS2, arrowhead marks the already formed posterior parakinetosomal structure (PPKS) next to KS2. **Fig. 13.** Detail of the preceding image. Arrowhead points at the PPKS, arrow marks cross-section of rootlet R5. n – nucleus; asterisk marks the base of the anterior flagellum. **Fig. 14.** A cell dividing into two future swarmers. At the posterior end there are still amoeboid projections. Arrows point at the kinetosome-microtubular associations. m – mitochondria. **Fig. 15.** A detail of the preceding picture, with the not yet fully formed microtubular structures. Arrowhead marks the PPKS, double arrows indicate cross-sectioned rootlet R5, thick arrow marks the rootlet R3. Microtubules of the outer cone R2 are marked by small arrows. KS1 and KS2 – kinetosomes of the anterior and posterior flagellum, respectively.

microtubular structures (Figs. 15, 22, 24, 25, 27, 28). Trophic stages possessing four flagella (obviously, stages in binary fission) that were regularly observed in the light microscope were also documented in thin sections (Figs. 14, 15). The two kinetosomes —given a suitable plane of section— were regularly observed at the same time. Both flagella, however, were only exceptionally seen in one section (Fig. 18).

Structural elements associated with kinetosomes of the flagellated swarmer stage already appeared in an indefinite position in the flagellated amoeba transforming into the swarmer. During the rapid proliferation rate of cells, their cytoskeletal elements were sometimes difficult to identify and trace in the course of morphogenesis. The metamorphosed swarmers had two kinetosomes in their apex, one longitudinally oriented, bearing the anterior flagellum (KS1), and a second one (KS2) with a flagellum extending postero-laterally. The KS2 sat with its base at the side of the anterior part of KS1. Associated with both kinetosomes were microtubules forming several systems —termed by previous authors as flagellum-cone, rootlet or outer and inner cone— and microfibrillar structures. To designate them, we use for simplicity the terminology based on Karpov and Mylnikov (1997) and Walker et al. (2003), i.e., rootlet 1 to 5, R1 to R5, although we realise, that e.g., the outer microtubular cone (R2) is in fact no rootlet.

The base of KS1 was linked by a thin microfibrillar band with a cluster of fibrillo-granular material, the microtubule organizing centre (MTOC) (Figs. 24, 25), from which microtubules emanate to form an inner microtubular cone around the nucleus, R1 (Fig. 16). The anterior end of the nucleus showed a more or less marked depression (Figs. 18, 21), above which a mass of Golgi vesicles or small cisternae was found. The largest microtubular system associated with KS1 was the outer microtubular cone (R2 flagellar cone of Schuster 1965). It extended in the cell periphery backwards (Figs. 16, 17, 21, 22, 28), reaching the level of the posterior end of the nucleus. These microtubules formed a loose corset. They were widely apart (about 180 nm) at the cell circumference (Figs. 16, 27) but not present around the whole cell. Up to 30 microtubules could be counted at the apex (Fig. 19) of the swarmer. Thus the anterior part of the nucleus is surrounded by a double microtubular basket. A one-layered ribbon or rootlet of microtubules, R3, 8 to 10 microtubules wide, arched around the KS1, subtending there microtubules of the outer cone (Figs. 21, 22, 28).

The KS2 was associated with two microtubular ribbons or rootlets, each bound to the opposite side of the kinetosome; one was a rootlet R4 composed of two microtubules originating at the posterior part of KS2, and crossed posteriorly the microtubules of the outer cone (Fig. 27, arrows). The other rootlet was a one-layered ribbon of 5 to 6 rather short microtubules (R5).

The array of these cytoskeletal structures was completed by the posterior parakinetosomal structure (PPKS) (term by Walker et al. 2003), consisting of two dense plates holding a network of fine fibres between them, the whole being attached to KS2 (Figs. 13, 26).

Sequence data and phylogenetic analyses

The sequences of SSU rDNA reported in this paper as newly obtained from clonal cultures of sea urchin strains are deposited in the GenBank database under accession numbers EF118757–EF118761. The length of these sequences ranged from 1910 to 1912 nt with GC contents 52.2–52.3%. The sequences of ECH49/I and ECH54/I were entirely identical; the dissimilarities calculated for sequences of these strains ranged from 0.01% (between ECH1/I and ECH43/I) up to 0.26% (between ECH1/I and ECH14/I). Within the whole dataset B (Fig. 30), the maximum percentage of sequence dissimilarity was found between the *Didymium squamulosum* and *D. iridis* (AJ938151) strains (17.65%) (Table 1).

The SSU rDNA-based phylogenetic reconstructions presented in Figs. 29 and 30 have shown that SUS form a separate, well-supported group, most closely related to *Hyperamoeba dachnaya*. In addition, the congruence of branching pattern within the datasets A (Fig. 29) and B (Fig. 30) clearly reflected a relatedness of SUS to strains of the genera *Didymium* and *Pseudodidymium* and to several strains assigned to *Hyperamoeba* (Hpl, E3P and E2/8). The maximum parsimonious tree (Fig. 29) has shown that the phylogenetic relationship of SUS and all other organisms included in the dataset A (strain representatives of several well-established myxogastrid genera and of some strains assigned to *Hyperamoeba*) is more distant.

DISCUSSION

In the beginning, phylogenetic analyses were included in this study just to verify a supposed identity of SUS with *Hyperamoeba flagellata* or *H. dachnaya*. Progress we have made in ultrastructural study of SUS revealed that at the moment the assignment of SUS to the genus *Hyperamoeba* would be supported only by the close relationship of SUS and *H. dachnaya* in the SSU rDNA tree, while other *Hyperamoeba* strains clustered with representatives of other genera.

Light microscopical and ultrastructural studies revealed similarities among SUS and species of the genera *Physarum* Persoon, 1794, *Didymium* Schrader, 1797, *Hyperamoeba* Alexeieff, 1923 and *Pseudodidymium* Michel, Walochnik et Aspöök, 2003. Representatives of these genera have been described with special respect to their ultrastructure by Schuster (1965), Wright et al. (1979), Michel et al. (2003), Walker et al. (2003), and Walochnik et al. (2004). To describe life-cycle stages of the organisms mentioned above, different terms have

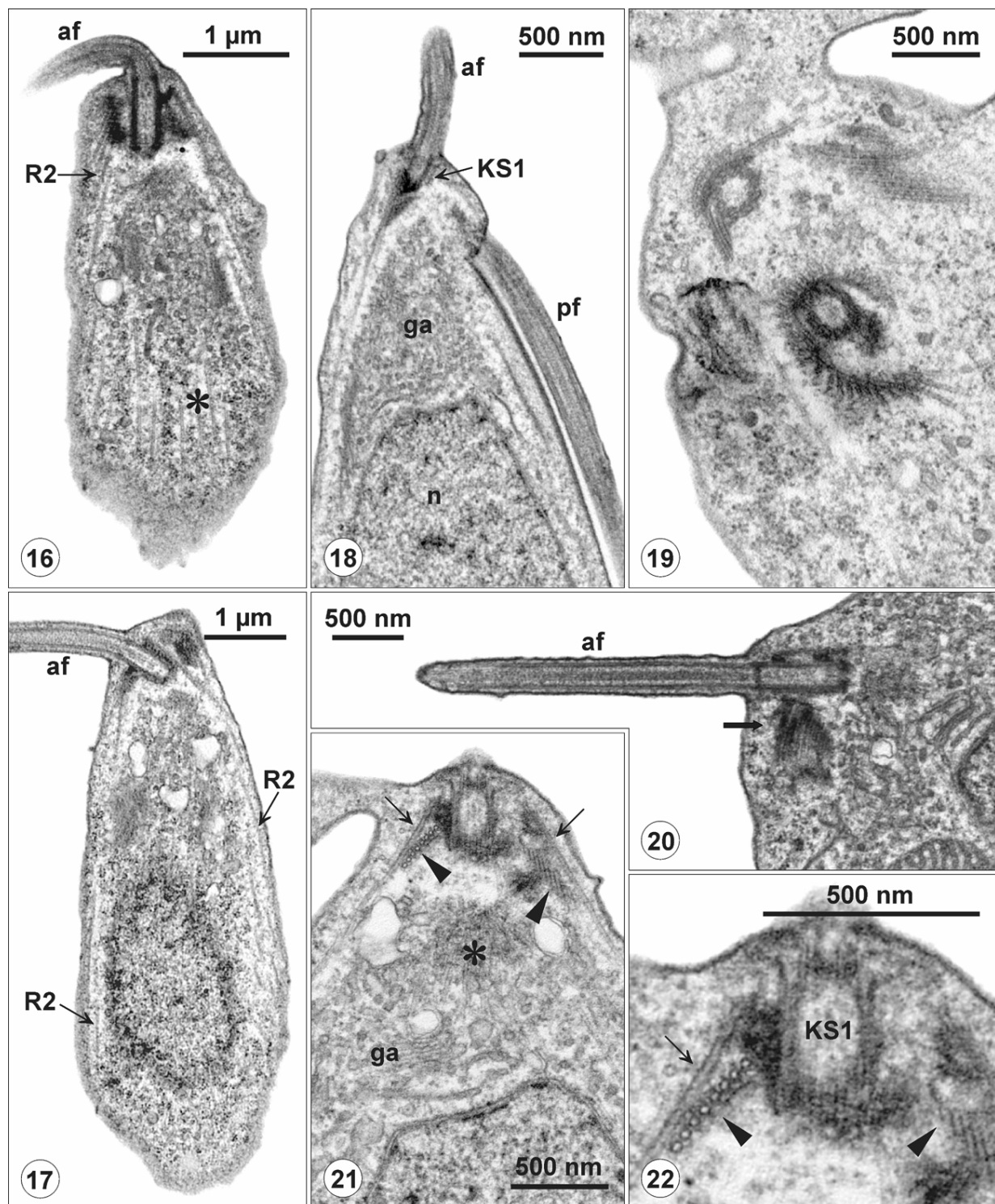


Fig. 16. Almost longitudinal section through the swarmer. af – anterior flagellum; R2 – microtubules of the outer cone; asterisk – microtubules of the inner cone R1. **Fig. 17.** Almost longitudinally sectioned swarmer. R2 – microtubules of the outer cone; af – anterior flagellum. **Fig. 18.** Anterior half of the swarmer, longitudinal section. af, pf – anterior and posterior flagellum; KS1 – kinetosome of the anterior flagellum; ga – Golgi apparatus; n – nucleus. **Fig. 19.** Apex of the cell forming two new swarmers with the kinetosome-microtubular complexes in formation. Only transverse sections of two KS1 are visible with distinct outer cone microtubules (R2). **Fig. 20.** Anterior flagellum (af) jutting out from the apex of the swarmer. Arrow marks the grazing section of KS2. **Fig. 21.** Section through the anterior end of a swarmer still with a cytoplasmic projection at left. Arrows point at microtubules of the outer cone encircling the KS1, arrowheads mark the R3 microtubules, asterisk marks the MTOC from which microtubules of the inner cone can be spotted, extending backwards; ga – Golgi apparatus. **Fig. 22.** Detail of the preceding figure with the same structures.

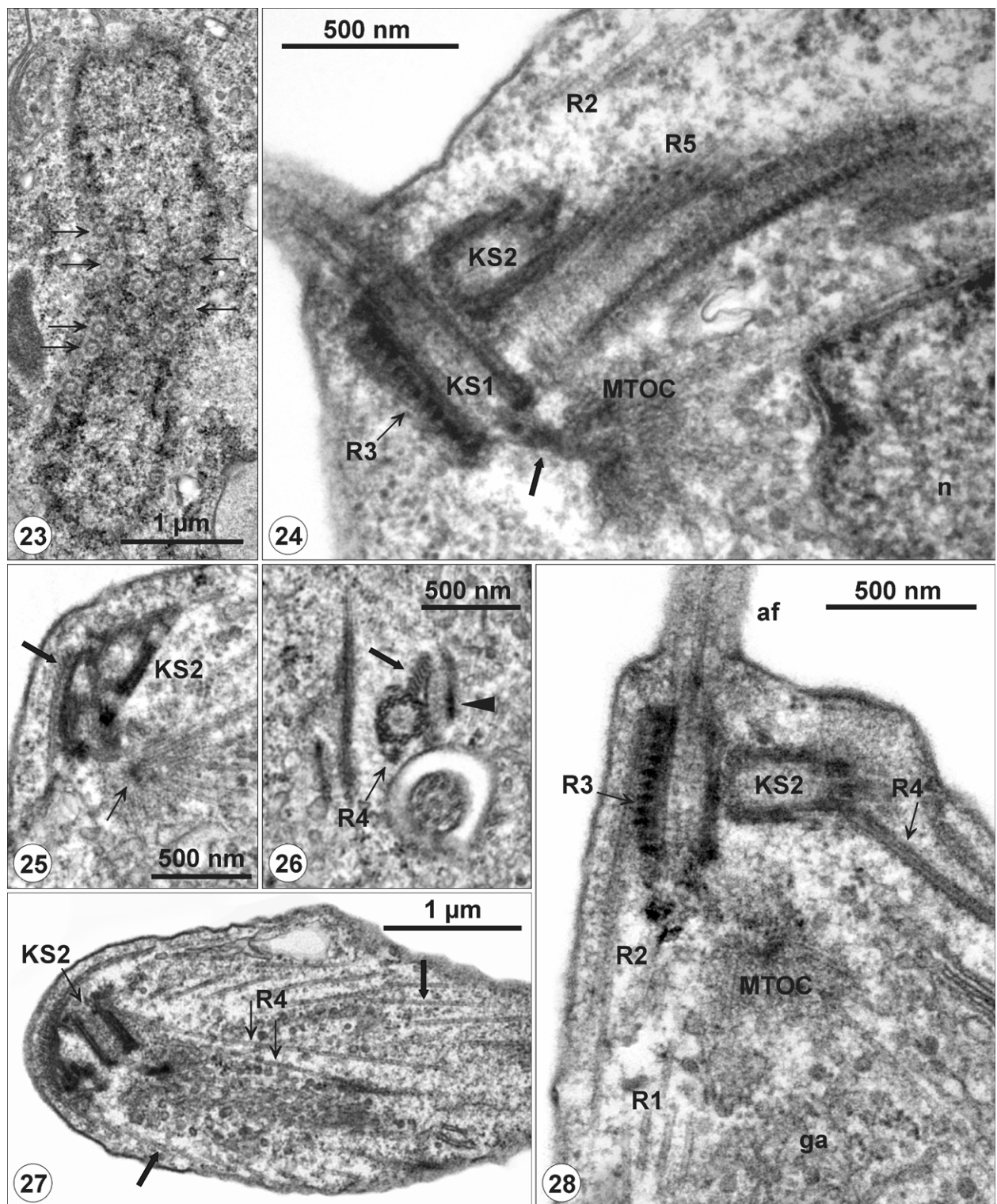


Fig. 23. Grazing section of the nucleus. Arrows mark the pores in the nuclear envelope. **Fig. 24.** Section through the apex of the swarmer with both kinetosomes visible. Arrow marks the thin microfibrillar link between the KS1 and MTOC, from which microtubules of the inner cone radiate; n – nucleus. **Fig. 25.** Two kinetosomes at the apex of the swarmer. Thick arrow points at the microtubules of the outer cone, thin arrow marks the MTOC giving rise to microtubules of the R1 rootlet. **Fig. 26.** Part of the apex of the swarmer showing KS2 in transverse section, the basal part of the anterior flagellum located in a pocket, PPKS, microtubular rootlet R4 (thick section) and doublet of R4. **Fig. 27.** Oblique section of the swarmer. KS2 situated next to the arc of microtubules of R2, extending backward (thick arrows). Two R4 microtubules are superimposed above the R2. **Fig. 28.** Apex of the swarmer with two kinetosomes. R4 microtubules extend from KS2; MTOC with radiating R1 microtubules; af – anterior flagellum; ga – Golgi apparatus.

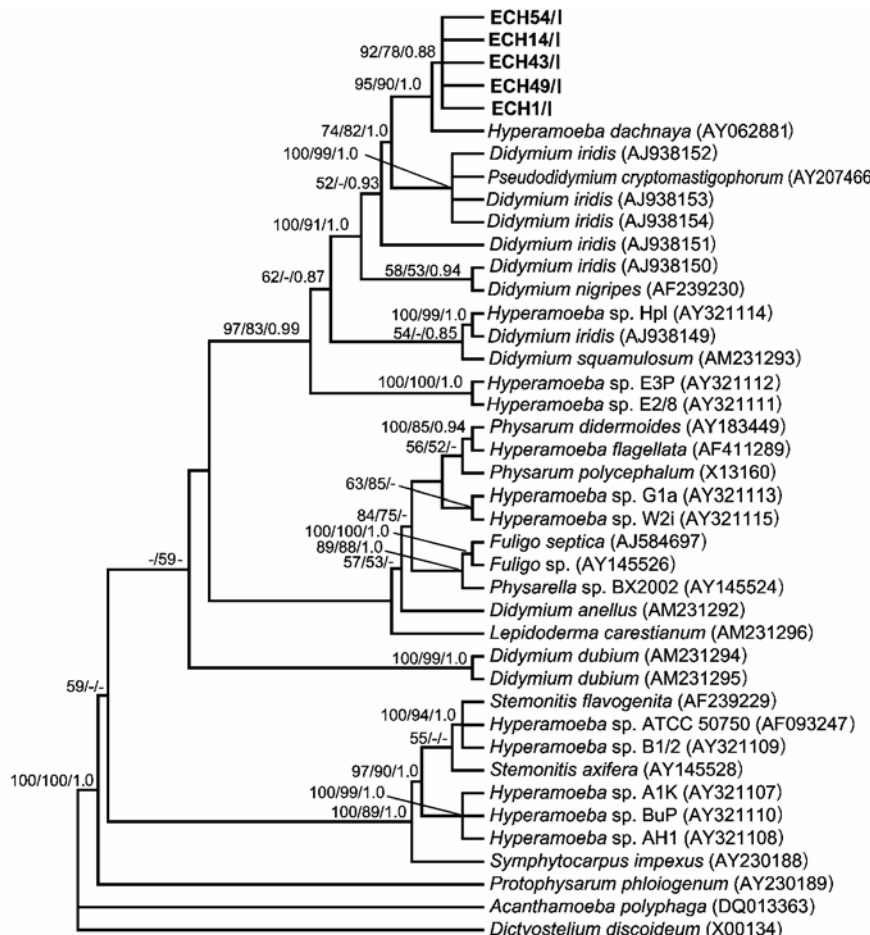


Fig. 29. Phylogenetic relationships among myxogastrids inferred from SSU rDNA sequences by the maximum parsimony method (strict consensus of 12 maximum parsimonious trees, Ts:Tv = 1:2, 3128 steps, CI = 0.58, RI = 0.74). *Acanthamoeba polyphaga* and *Dictyostelium discoideum* were set as outgroup species. Numbers at the nodes represent the bootstrap values (MP and ML; shown >50% support) and BI posterior probabilities. GenBank accession numbers are in parentheses.

been used: a uninucleate amoeboid stage (myxamoeba, amoeba) for stages resembling trophic stages of free-living amoebae, or, swarm cell (swarmer, amoeboid flagellate, amoeboflagellate, flagellate) for fast-moving small flagellated stages, or, cysts or microcysts for encysted stages. The organisms isolated from sea urchins concur with *D. nigripes*, *H. dachnaya*, *H. flagellata* and *Pseudodidymium cryptomastigophorum* in their ability to transform into three forms, a trophic stage (myxamoeba), a flagellate (swarm cell), and cyst. Corresponding stages were recognized easily and their ultrastructure could be compared. The formation of fruiting bodies was observed neither in SUS, nor in *H. dachnaya* and *P. cryptomastigophorum* compared in the study and cultured under different conditions, while *Physarum polycephalum* and *D. nigripes* are well known to produce plasmodia and fruiting bodies under appropriate conditions.

Looking for the possible identity of SUS, comparison of trophic (amoeboid) stages was of no great help due to changeability of these stages and transient character of their pseudopodia. Nuclear division of amoeba stages in

SUS proceeded, similarly as in *Didymium nigripes* myxamoebae (Schuster 1965), as an open mitosis. This does not help either in revealing the identity of SUS. The swarmer fine structure may be instrumental in revealing the taxonomic affinities of the SUS. The SUS cytoskeleton has some features in common with almost all above-mentioned organisms. They have five types of microtubular rootlets, the MTOC connected with the flagellum-bearing kinetosome and the curious posterior parakinetosomal structure. It is quite similar to what has been found in representatives of the class Protostelea (Spiegel 1981, 1982). However, swarmers of *Physarum polycephalum* have a rather extensive outer microtubular cone. In addition, the above mentioned group of organisms differs from protostelids by the structure of their mitochondria. In SUS, as well as in *H. dachnaya*, *H. flagellata*, *Didymium* spp. and *P. cryptomastigophorum*, mitochondria have an electron-dense core oriented in their long axis. The presence of filamentous nucleoid mentioned as a feature proper to Myxogastrea (Schuster 1965, Guttes et al. 1966) is not in favour of SUS being related to protostelids.

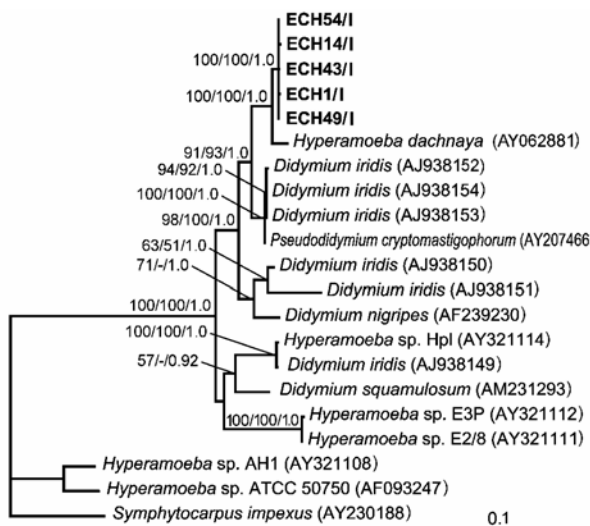


Fig. 30. Maximum likelihood tree ($-ln= 12435.9626$) of SSU rDNA sequences of sea-urchin strains and closely related myxogastrids. *Sympylocarpus impexus*, *Hyperamoeba* sp. AH1 and *Hyperamoeba* sp. ATCC 50750 were set as outgroup species. The bootstrap values (MP and ML) gaining more than 50% support and BI posterior probabilities are indicated at the nodes. GenBank accession numbers are in parentheses. Scale bar is given under the tree.

In spite of the fact that in the phylogenetic analyses based on SSU rDNA sequences, SUS were found to be the closest relatives of *H. dachnaya*, the difference in ultrastructure of swarmer stages and in the number of flagella prevent us from identifying SUS with this species. *Hyperamoeba dachnaya* (as well as *H. flagellata* with more distant phylogenetic position) was described as having one well-developed flagellum in the swarmer stage. The difference in cyst morphology (*H. dachnaya* bears dense outgrowths forming a surface layer of small compartments) was considered of less importance. Since also other representatives of strongly supported cluster containing SUS (Fig. 30), e.g., *D. nigripes* and *Pseudodidymium cryptomastigophorum*, ultrastructure of which has been studied in detail, have swarmers with two flagella, a serious doubt persists whether the second flagellum could not be overlooked in *Hyperamoeba* spp., especially, where the presence of two kinetosomes was documented. This is an obvious question since we have experienced how decisive in understanding the ultrastructure of flagellar apparatus is the level of section and since we faced difficulties trying to obtain convincing documentation of both flagella.

In addition to the presence of one or two flagella that seems essential when relevant life-cycle stages are compared, there are also differences in microtubular rootlets associated with kinetosomes. Contrary to SUS, the rootlet associated with KS2 in *P. cryptomastigophorum* consists of a double layer of microtubules. Although the basic plan of the cytoskeleton is comparable, its ar-

angement in swarmers of *H. dachnaya* and *H. flagellata* is different.

In *D. nigripes* swarmers possessing two flagella like in SUS, Schuster (1965) described only the outer microtubular cone (i.e., flagellar cone). However, in his figs. 22 and 26 one can decipher below the flagellum-bearing kinetosome a MTOC, from which microtubules of the inner microtubular cone radiate. Thus it is quite probable that the other constituents of the cytoskeleton were also present, considering that Schuster (1965) in the same paper also published electron micrographs of *Physarum polycephalum* in which he did not reveal all rootlets described in *P. polycephalum* by Wright et al. (1979).

Despite the fact that we did not observe plasmodial stages or sorocarps, i.e., spore-to-spore culturing was not accomplished in SUS, the study of ultrastructure and phylogeny revealed an incontestable kinship with *Didymium*. The lack of sorocarp formation was mentioned several times in myxogastrids cultured on agar (Karpov and Mylnikov 1997, Michel et al. 2003), however, structurally similar fruiting bodies are considered typical feature of Myxogastrea (Frederick 1990). We think it premature to assign the SUS strains as a species to *Didymium* or to establish it as a new genus. We propose for the time being to consider SUS as *Didymium*-like myxogastrids and postpone establishment of new genus or species until ultrastructural studies of other phylogenetically related organisms are completed. This should also include the comparison of SSU rDNA based phylogeny with phylogeny inferred from different molecular markers (Fiore-Donno et al. 2005). This approach might help to recognise the importance of ultrastructure of flagellar apparatus at the generic or specific level and of course also add some data to the knowledge of evolution of this apparatus.

Broad evaluation of phylogenetic relationships within datasets of mycetozoan sequences is out of the scope of this study. However, some comments can be added regarding results presented in previous papers analysing limited datasets of myxogastrids. Phylogenetic analyses supported the results obtained by Walochnik et al. (2004). Sequences of the same *Hyperamoeba* strains clustered together while others formed tree branches in clusters belonging to two different orders. Re-examination of generic assignment of *Hyperamoeba* strains included in phylogenetic analyses is desirable in order to prepare a solid base for phylogenetic conclusions.

To the best of our knowledge, considering the most diverse microhabitats from which the compared myxogastrean strains originated, this is a first report of a myxogastrid as an endocommensal of sea urchins. Evidently, myxogastrids have a broad ecological potential, as they were already found also in mire, tree bark, horse faeces and spa bath. In this sense they may exceed other Amoebozoa or Heterolobosea.

Table 1. Percentage of sequence dissimilarities among myxogastrid sequences inferred from alignment B (without intron sequences in sequences of *P. cryptomastigophorum*, *D. squamulosum*, *D. nigripes* and four sequences of *D. iridis* (Acc. Nos. AJ938150, AJ938151, AJ938153 and AJ938154).

	1	2	3	4	5	6	7	8	9	10	11	12	13	14	15	16	17	18	19	20	21
1 ECH54/I		0																			
2 ECH49/I		0.00	0																		
3 ECH1/I		0.10	0.10	0																	
4 ECH43/I		0.05	0.05	0.01	0																
5 ECH14/I		0.16	0.16	0.26	0.21	0															
6 AY062881 <i>H. dachnaya</i>	2.09	2.09	2.19	2.14	2.25	0															
7 AJ938152 <i>D. iridis</i>	3.91	3.91	4.02	3.96	4.07	4.58	0														
8 AJ938153 <i>D. iridis</i>	3.71	3.71	3.82	3.76	3.86	4.40	0.16	0													
9 AJ938154 <i>D. iridis</i>	3.75	3.75	3.86	3.80	3.91	4.40	0.16	18.76	0												
10 AY207466 <i>P. cryptomastigophorum</i>	3.63	3.63	3.74	3.68	3.79	4.29	0.32	0.15	0.16	0											
11 AJ938150 <i>D. iridis</i>	5.70	5.70	5.82	5.75	5.87	6.04	5.16	5.02	5.01	4.92	0										
12 AF239230 <i>D. nigripes</i>	5.76	5.76	5.87	5.81	5.92	6.19	5.34	5.40	5.41	5.36	7.75	0									
13 AJ938151 <i>D. iridis</i>	6.83	6.83	6.94	6.88	7.00	7.42	6.68	6.64	6.65	6.77	11.31	13.40	0								
14 AY321114 <i>Hyperamoeba</i> sp. Hpl	7.57	7.57	7.68	7.62	7.73	8.69	7.32	7.28	7.36	7.29	7.51	7.52	9.02	0							
15 AJ938149 <i>D. iridis</i>	7.64	7.64	7.75	7.69	7.80	8.46	7.39	7.39	7.47	7.41	7.39	7.53	9.02	0.21	0						
16 AM231293 <i>D. squamulosum</i>	7.52	7.53	7.64	7.58	7.69	8.08	7.27	7.26	7.31	7.18	16.61	17.28	17.65	6.47	6.04	0					
17 AY321112 <i>Hyperamoeba</i> sp. E3P	9.66	9.62	9.78	9.72	9.83	10.37	9.05	8.87	8.92	8.75	10.18	10.44	11.40	8.95	9.07	8.44	0				
18 AY321111 <i>Hyperamoeba</i> sp. E2/8	9.51	9.52	9.62	9.56	9.67	10.22	8.89	8.71	8.77	8.59	10.01	10.45	11.40	8.79	8.96	8.28	0.16	0			
19 AY321108 <i>Hyperamoeba</i> sp. AH1	16.95	16.97	17.07	17.01	17.01	17.49	17.23	17.28	17.43	17.24	17.03	17.44	18.45	16.97	17.34	16.99	17.03	16.87	0		
20 AF093247 <i>Hyperamoeba</i> sp.	17.42	17.44	17.54	17.47	17.47	18.18	17.05	16.99	17.15	16.94	17.01	16.92	18.76	16.90	17.27	16.86	16.77	16.62	5.69	0	
21 AY230188 <i>S. impexus</i>	17.43	17.44	17.54	17.48	17.48	18.02	17.65	17.55	17.78	17.41	17.58	17.88	19.11	16.60	17.02	16.82	18.08	17.92	11.12	11.62	0

Results of this study raised questions regarding generic and species definitions and phylogenetic relationships within mixed clusters of organisms, which the study of additional species and isolates might resolve. We suppose that a revision is warranted of these myxogastrid organisms which would embrace ultrastructure, molecular analysis and certainly life cycle studies and ecological potential. The re-examination of nuclear phenomena in myxogastrids would also be worth of study. Two types of nuclear division observed in the life cycle of *Didymium* are quite unusual. Similarly as *Didymium* myxamoebae observed by Schuster

(1965), trophozoites of *Didymium*-like organisms from sea urchins revealed an open mitosis.

Acknowledgements. We want to thank Dr. Oleg Ditrich for collecting the urchins during the field Course of Marine Invertebrate Biology organised by the Faculty of Biological Sciences, University of South Bohemia. The study was supported by the National Science Foundation of the Czech Republic (Project No. 206/05/2384), Ministry of Education, Youth and Sports (Project No. MSM6007665801), the Research Centre "Ichthyoparasitology" (LC522) and by the research project of the Institute of Parasitology, Biology Centre, Academy of Sciences of the Czech Republic (Z60220518).

REFERENCES

DYKOVÁ I., PECKOVÁ H., FIALA I., DVOŘÁKOVÁ H. 2005a: *Filamoeba sinensis* sp. n., a second species of the genus *Filamoeba* Page, 1967, isolated from gills of *Carassius gibelio* (Bloch, 1782). *Acta Protozool.* 44: 75–80.

DYKOVÁ I., PECKOVÁ H., FIALA I., DVOŘÁKOVÁ H. 2006: Fish-isolated *Naegleria* strains and their phylogeny inferred from ITS and SSU rDNA sequences. *Folia Parasitol.* 53: 172–180.

DYKOVÁ I., PINDOVA Z., FIALA I., DVOŘÁKOVÁ H., MACHÁČKOVÁ B. 2005b: Fish-isolated strains of *Hartmannella vermiformis* Page, 1967: morphology, phylogeny and molecular diagnosis of the species in tissue lesions. *Folia Parasitol.* 52: 295–303.

FOIRE-DONNO A.M., BERNEY C., PAWLOWSKI J., BALDAUF S.L. 2005: Higher-order phylogeny of plasmodial slime molds (Myxogastria) based on elongation factor 1-A and small subunit rRNA gene sequences. *J. Eukaryot. Microbiol.* 52: 201–210.

FREDERICK L. 1990: Phylum Plasmodial Slime Molds – Class Myxomycota. In: L. Margulis, J.O. Corliss, M. Melkonian and D.J. Chapman (Eds.), *Handbook of Protocista*. Jones and Bartlett, Boston, pp. 467–483.

GUTTES S., GUTTES E., HADEK R. 1966: Occurrence and morphology of a fibrous body in the mitochondria of the slime mould *Physarum polycephalum*. *Experientia* 22: 452–454.

JONES G.M. 1985: *Paramoeba invadens* n. sp. (Amoebidae, Paramoebidae), a pathogenic amoeba from the sea urchin, *Strongylocentrotus droebachiensis*, in Eastern Canada. *J. Protozool.* 32: 346–369.

KARPOV S.A., MYLNIKOV A.P. 1997: Ultrastructure of the colourless flagellate *Hyperamoeba flagellata* with special reference to the flagellar apparatus. *Eur. J. Protistol.* 33: 349–355.

MICHEL R., WALOCHNIK J., ASPÖK H. 2003: *Pseudodidymidium cryptomastigophorum* gen. n., sp. n., a *Hyperamoeba* or a slime mould? A combined study on morphology and 18S rDNA sequence data. *Acta Protozool.* 42: 331–343.

MULLEN T.E., NEVIS K.R., O'KELLY C.J., GAST R.J., FRASCA S. Jr. 2005: Nuclear small-subunit ribosomal RNA gene-based characterization, molecular phylogeny and PCR detection of the *Neoparamoeba* from Western Long Island Sound lobster. *J. Shellfish Res.* 24: 719–731.

MULLEN T.E., RUSSEL S., TUCKER M.T., MARATEA J.L., KERTING C., HINCLEY L., DE GUISE S., FRASCA S. Jr., FRENCH R.A. 2004: Paramoebiosis associated with mass mortality of American lobster *Homarus americanus* in Long Island Sound, USA. *J. Aquat. Anim. Health* 16: 29–38.

RONQUIST F., HUELSENBECK J.P. 2003: MrBayes 3: Bayesian phylogenetic inference under mixed models. *Bioinformatics* 19: 1572–1574.

SCHUSTER F.L. 1965: Ultrastructure and morphogenesis of solitary stages of true slime molds. *Protistologica* 1: 49–62.

SPIEGEL F.W. 1981: Phylogenetic significance of the flagellar apparatus in protostelids (Eumycetozoa). *Biosystems* 14: 491–499.

SPIEGEL F.W. 1982: The ultrastructure of the trophic cells of the protostelid *Planoprotostelium aurantium*. *Protoplasma* 113: 165–177.

SWOFFORD D.L. 2001: PAUP*: Phylogenetic Analysis Using Parsimony (*and other methods). Version 4.0b10. Sinauer Associates, Sunderland, Massachusetts, USA.

THOMPSON J.D., GIBSON T.J., PLEWNIAK F., JEANMOUGIN F., HIGGINS D.G. 1997: The CLUSTAL_X windows interface: flexible strategies for multiple sequence alignment aided by quality analysis tools. *Nucl. Acids Res.* 25: 4876–4882.

WALKER G., SILBERMAN J.D., KARPOV S.A., PREISFELD A., FOSTER P., FROLOV A.O., NOVOZHILOV Y., SOGIN M. 2003: An ultrastructural and molecular study of *Hyperamoeba dachnaya*, n. sp., and its relationship to the mycetozoan slime moulds. *Eur. J. Protistol.* 39: 319–336.

WALOCHNIK J., MICHEL R., ASPÖK H. 2004: A molecular biological approach to the phylogenetic position of the genus *Hyperamoeba*. *J. Eukaryot. Microbiol.* 51: 433–440.

WRIGHT M., MOISAND A., MIR L. 1979: The structure of the flagellar apparatus of the swarm cells of *Physarum polycephalum*. *Protoplasma* 100: 231–250.

Received 14 November 2006

Accepted 15 January 2007